

Supporting Information

pH Responsive Dual Cargo Delivery from Mesoporous Silica Nanoparticles with a Metal-latched Nanogate

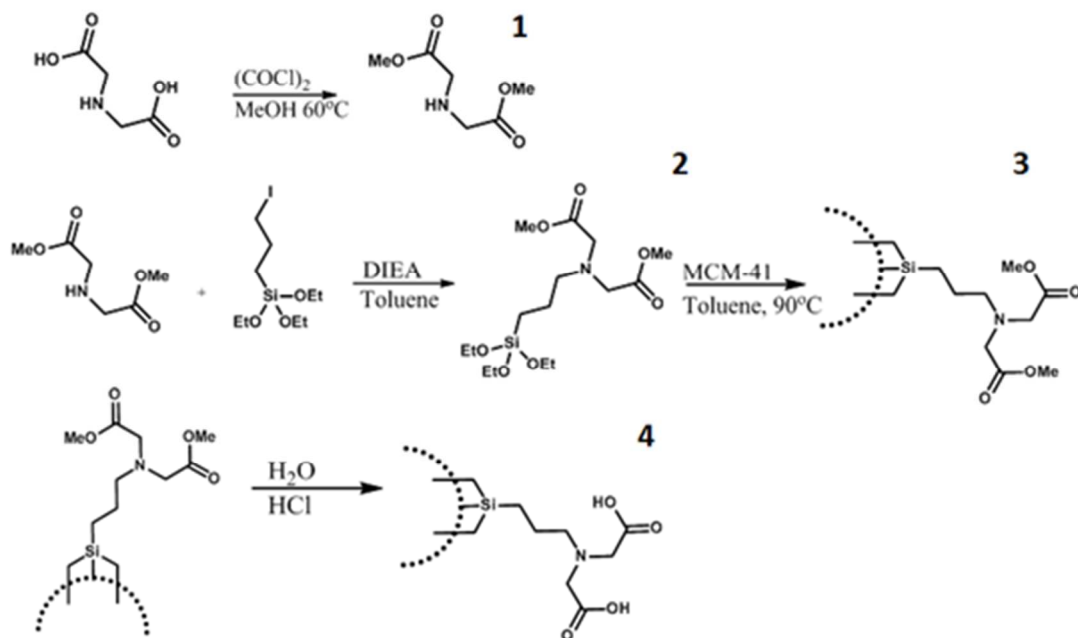
Derrick Tarn, Min Xue, and Jeffrey I. Zink

Department of Chemistry and Biochemistry, California NanoSystems Institute,

University of California, Los Angeles, California 90095, United States

Table of Contents

Scheme 1. Synthesis and attachment of nanogate -----	3
Figure S1. TEM image of MCM-41 nanoparticles -----	4
Figure S2. XRD powder diffraction of MSN -----	5
Figure S3. Infrared spectrum of template extracted MSN -----	5
Figure S4a. SS ¹³ C NMR spectrum of iminodiacetic acid modified MSN -----	6
Figure S4b. SS ²⁹ Si NMR spectrum of iminodiacetic acid modified MSN -----	6
Figure S5. Time-resolved fluorescence spectrum of competitively binding released nickel(II) latched nanogates -----	7
Figure S6. UV-Vis spectra of solution Co/EDTA complexes after simulated loading conditions -----	8
Figure S7. Experimental setup for time-resolved fluorescence spectroscopy -----	8
Figure S8. UV-Vis spectra of CoCl ₂ and CoCl ₂ after being coordinated with IDA -----	9



Scheme S1. Synthesis and attachment of nanogate machine.

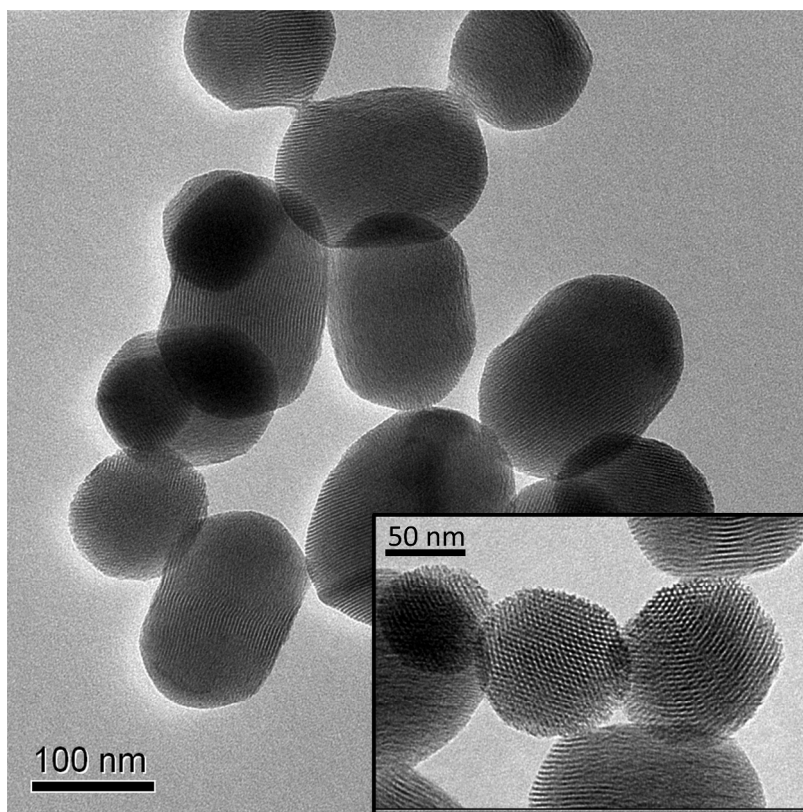


Figure S1. TEM image of a typical batch of synthesized and acid extracted MCM-41 nanoparticles.

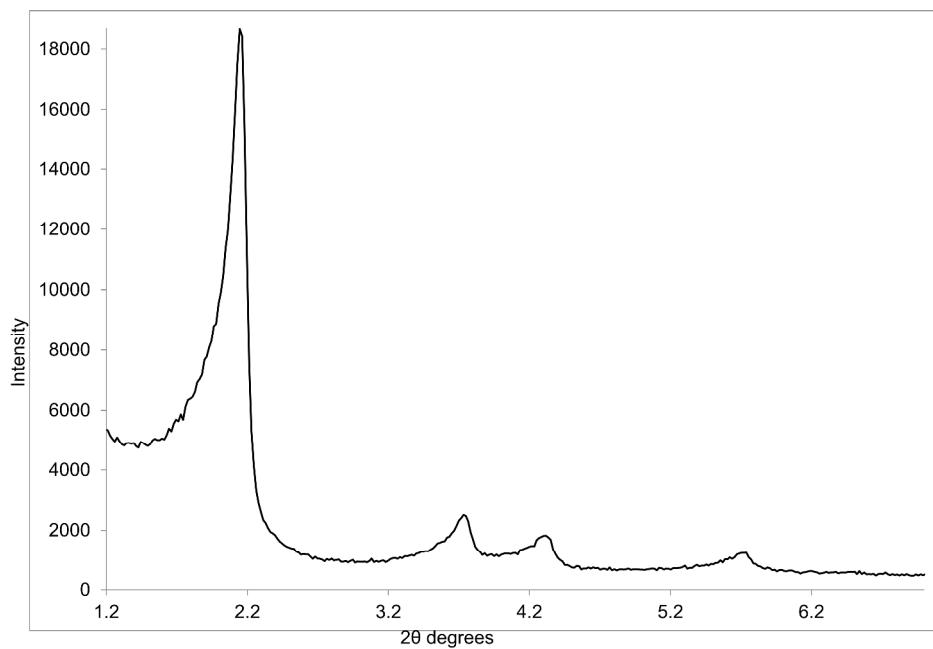


Figure S2. Powder XRD diffraction of synthesized MCM-41 nanoparticles.

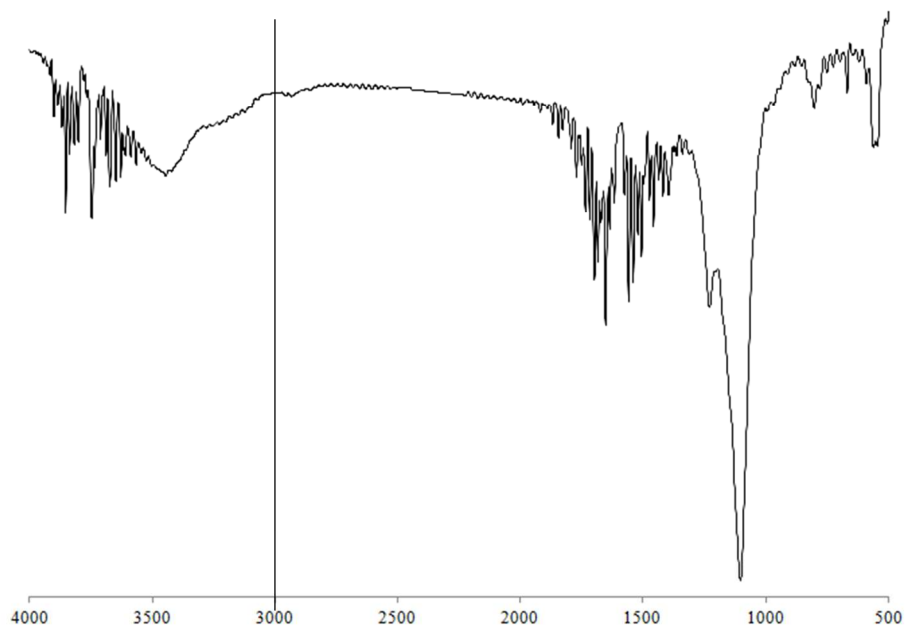


Figure S3. IR of surfactant extracted synthesized MSN.

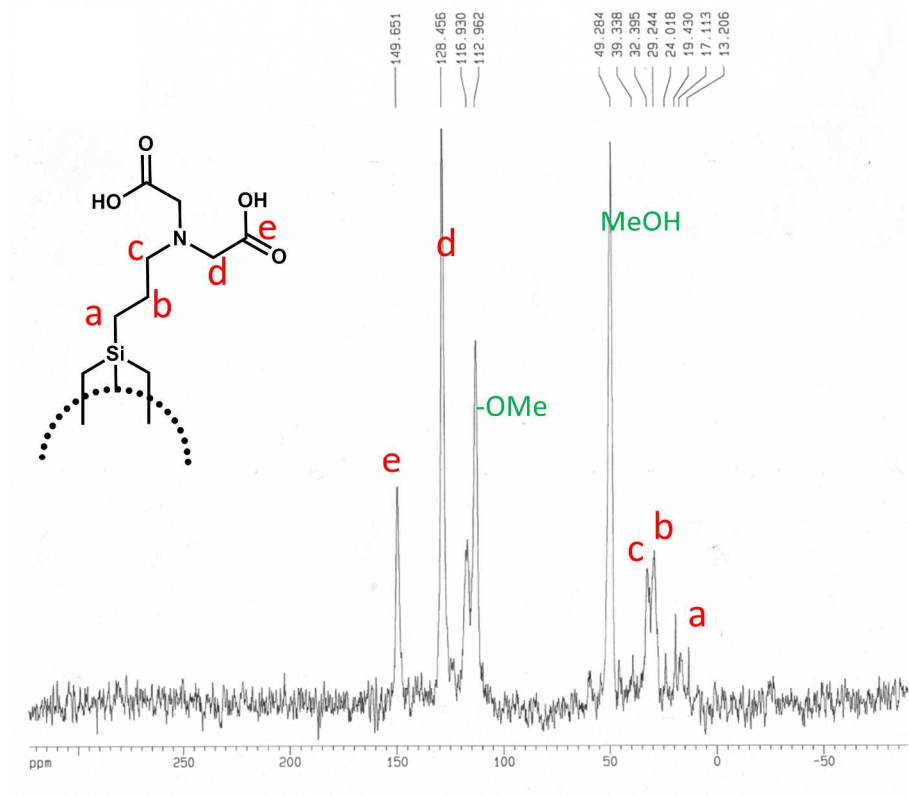


Figure S4a. SS ^{13}C NMR spectrum of iminodiacetic acid modified MSN. Peaks corresponding to IDA are observed in the region >50 ppm. Bare nanoparticles with $-\text{OMe}$ terminated silanes do not show peaks in this region.

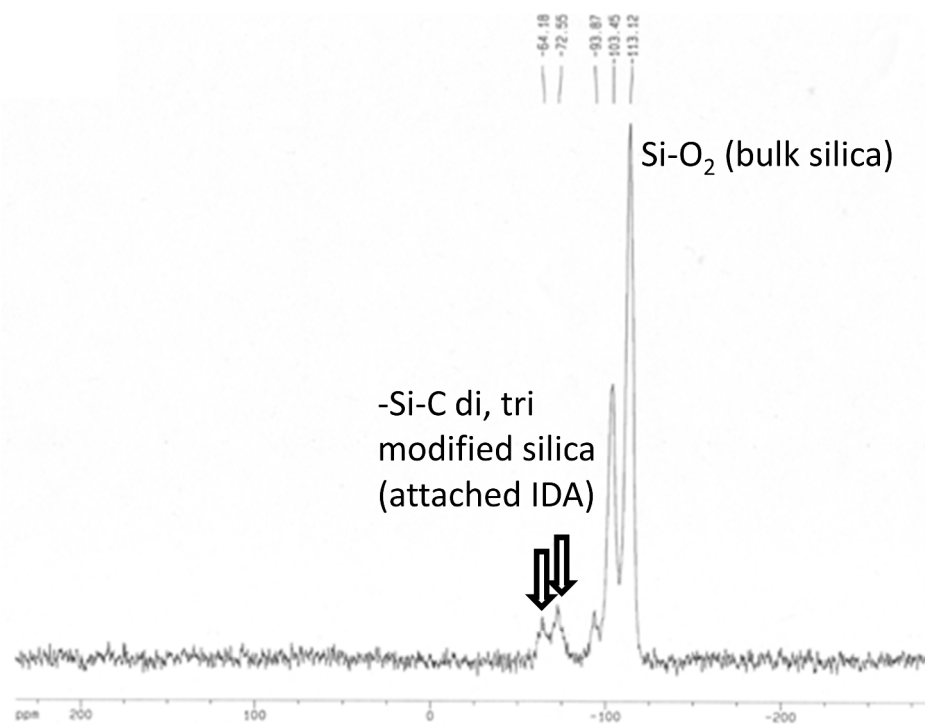


Figure S4b. SS ^{29}Si NMR spectrum of iminodiacetic acid modified MSN.

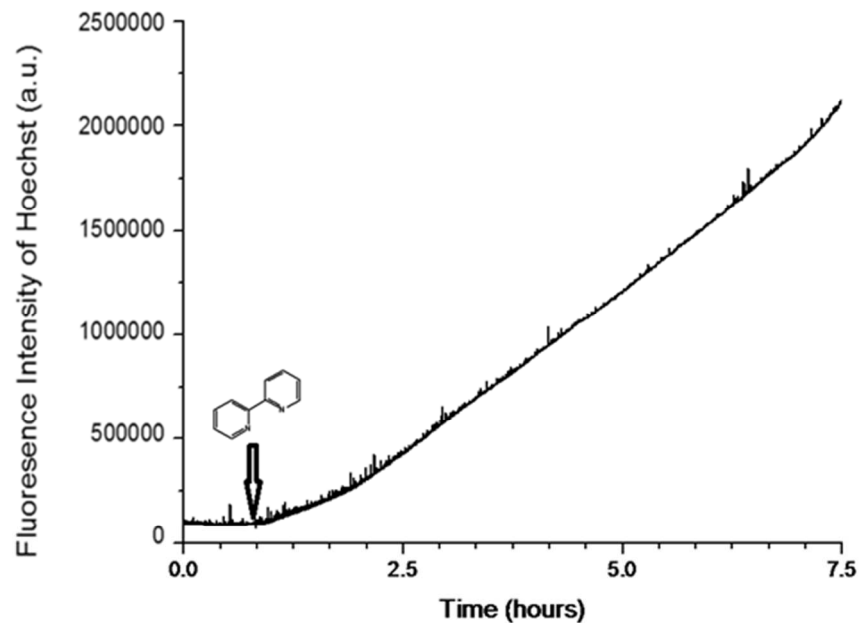


Figure S5. Time resolved fluorescent spectrum release profile of Hoechst 33342 cargo from a nickel latched nanogate machine. Solid 2,2'-bipyridine was added as a competitively binding ligand to remove nickel from the iminodiacetic acid nanogates and initiate cargo release. The slow rate of release was due to the low solubility of 2,2'-bipyridine in water.

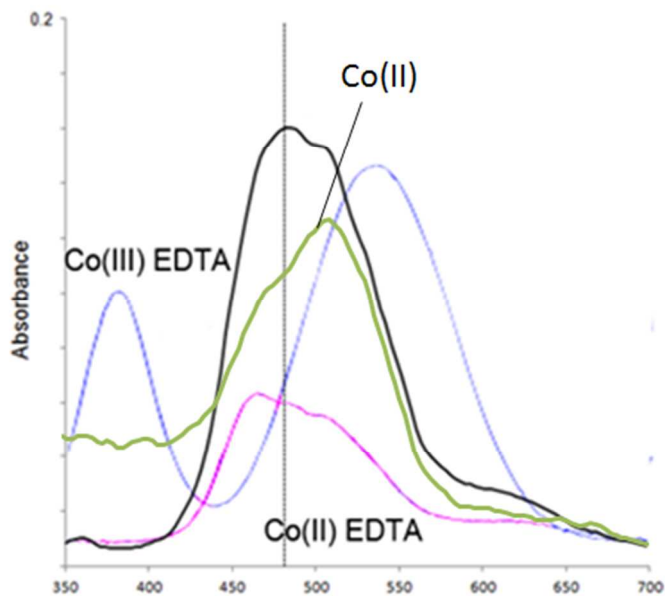


Figure S6. UV-Vis spectra of solution Co/EDTA complexes after simulated loading conditions. The oxidation state of cobalt was determined through spectroscopic methods after mimicking the loading and capping conditions of the nanoparticles. In green: UV-Vis spectra of a Co(II) solution in water. In pink: UV-Vis spectra of 5 mM Co(II)EDTA. In blue: Co(III)EDTA complex (Xue, Y.; Traina, S. *J. Environ. Sci. Technol.* **1996**, 30, 1975-1981). In black: UV-VIS spectra of 10 mM cobalt/EDTA complex after undergoing similar conditions as used in the loading/capping procedures. After this process, the cobalt is bound to EDTA as shown in the increase in absorbance at 470 nm, and most of the cobalt/EDTA is still in the +2 oxidation state as indicated by the absence of a peak at 370 nm.

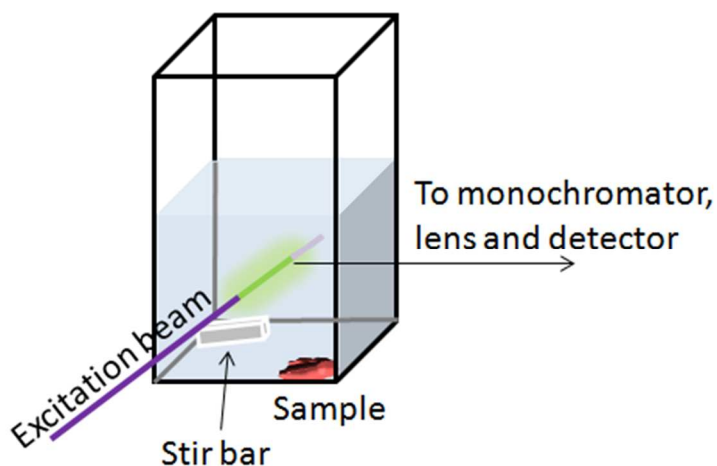


Figure S7. Experimental setup for time-resolved fluorescence spectroscopy. An excitation beam is aimed at the solution supernatant, exciting any dye molecules present. A CCD detector cooled to liquid nitrogen temperatures integrates intensities at a specified wavelength in real-time to generate a typical release profile curve.